only for small N, and as the latter increases, the differences between the curves become slight, and they rapidly approach the asymptote $e_p^* = 2/N$ indicated by the points in Fig. 6.

As an example we consider the flow of an aerosol between two grounded grids separated by L = 0.1 m. The flow speed is 4.5 m/sec and the conditions [4] are $a = 2.2 \cdot 10^{-5}$ m, $n_p = 2 \cdot 10^{-10}$ m^{-3}, $D = 10^{-5}$ m^2/sec, $b = 2 \cdot 10^{-4}$ m^2(V·sec).

Here Pe = 10 and N = 1, 3. At saturation, the transport current density is $1.5 \cdot 10^{-5}$ A/m^2, while the particle charge at the collector is $2 \cdot 10^{-16}$ C. If under otherwise constant conditions the particle concentration is reduced to $n_p = 10^7$ m^{-3}, the effects from the particles on the flow become negligible and the transport current density falls to 10^{-5} A/m^2, while the particle charge rises to $5 \cdot 10^{-16}$ C.

LITERATURE CITED

1. S. Sou, Charged-Suspension Dynamics [Russian translation], Mir, Moscow (1975).
2. G. L. Sedova and L. T. Chernyi, "The electrohydrodynamic equations for weakly ionized aerosols showing dispersed-phase particle charging by diffusion," Izv. Akad. Nauk SSSR, Mekh. Zhidk. Gaza, No. 1 (1986).
3. A. V. Filippov, "Aerosol-particle charging in an electric field with allowance for ion diffusion," Izv. Akad. Nauk SSSR, Mekh. Zhidk. Gaza, No. 1 (1986).
4. A. B. Vatazhin, V. I. Grabovskii, V. A. Likhter, and V. I. Shul'gin, Electro-Gas Dynamic Flows [in Russian], Nauka, Moscow (1983).
5. V. V. Ushakov and G. M. Franchuk,"Aerosol particle charging in a one-dimensional electro-gas dynamic flow," Magn. Gidrod., No. 2 (1973).
6. N. L. Vasil'eva and L. T. Chernyi, "Aerosol particle electrification on motion in a one-dimensional corona discharge," Zh. Prikl. Mat. Tekh. Fiz., No. 4 (1982).
7. A. N. Nayfeh, Perturbation Methods, Wiley, New York (1973).
8. J. D. Klett, "Ion transport to cloud droplets by diffusion and conduction and the resulting droplet charge distribution," J. Atmos. Sci., 28, 78 (1971).
9. N. L. Vasil'eva, G. L. Sedova, A. V. Filippov, and L. T. Chernyi, "Electrohydrodynamic flows of weakly ionized aerosols involving dispersed-phase particle charging," in: Abstracts for the 6th All-Union Congress on Theoretical and Applied Mechanics [in Russian], Tashkent (1986).

STUDY OF A SHOCK WAVE IN A TUBE PRODUCED BY A SPHERICAL EXPLOSION

É. K. Anderzhanov and B. D. Khristoforov

UDC 533.6.011

Empirical expressions were obtained in [1] for parameters of shock waves produced in tubes by explosion of concentrated explosive charges in air, valid for large distances from the center of the explosion, where the piston action of the products can be neglected and the spherical shock wave transforms to planar. Below we will present results of an experimental study of the explosion near-zone. Numerical solution of such a three-dimensional nonlinear nonsteady-state problem is made difficult by the need to consider the complex pattern of interaction of the direct shock wave and reflections from the tube walls, the hydrodynamic instabilities which then develop on the tube axis, and the real properties of the medium, which consists of air mixed with explosion products due to Rayleigh–Taylor instability.

Metallic tubes with radii r = 1.5 and 1.9 cm were used in the experiments, with spherical TEN charges of mass M = 0.8 and 2.5 g ($\rho = 1.6$ g/cm^3) being detonated on the tube axis. Initiation was accomplished in the center of the charge, using a small amount of lead azide and electrical explosion of a 0.05-mm thick manganin wire penetrating the charge.

The motion of the shock-wave front was photographed by an SFR-2M camera attached to a shadow device through a rectangular window in the tubes in a photorecorder regime. Shock-wave exit from tubes of various length and the hydrodynamnic flow pattern were recorded in

Moscow. Translated from Zhurnal Prikladnoi Mekhaniki i Tekhnicheskoi Fiziki, No. 5, pp. 25-27, September-October, 1988. Original article submitted March 16, 1987.

0021-8944/88/2905-0622$12.50

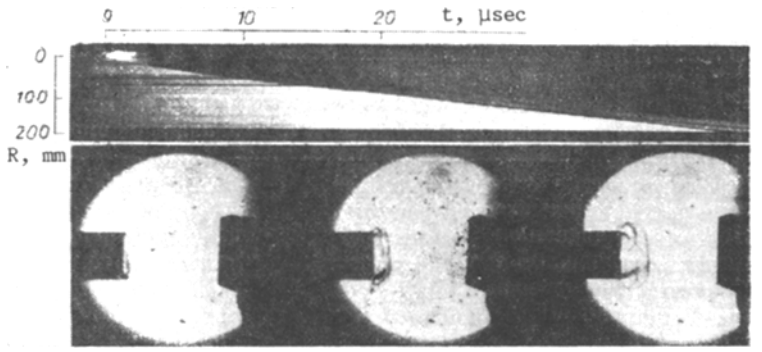

Fig. 1

a time loop mode. These data were used to construct hodographs of R(t) of the shock-wave front in the tubes and determine its parameters. In processing the experimental results scattering of the explsoive layers, which for the charges used comprised ~0.2 mm [2], was considered.

Figure 1 shows photographs of the shock wave in the tube as obtained by the slit method and frame-by-frame photography (to the right in the frames one can see the mirror used to record the time of initiation, time between exposures, 4 μsec), while Figs. 2-4 present shock-wave hodographs for various explosion conditions. To clarify the conditions of shock-wave formation in the tube and to determine empirical expressions for the front parameters the measured hodographs were compared to ones obtained for a TEN explosion in an unbounded atmosphere [2] and hodographs of a shock wave in a tube calculated from the latter with the assumption that front parameters are a function of the ratio of the explosive energy (or mass) to the mass of air in the shock wave, and are independent of the explosion symmetry. For a Sedovskii explosion this assumption is strictly satisfied, while for detonation of an explosive charge it is satisfied approximately [3].

The parameter which was varied in recalculating the data of [2] was the position of the boundary R_1 for transition from spherical to planar symmetry which can be estimated from the experimental results (Figs. 2-4) from the point where the measured hodograph (circles) diverges from the hodograph for a spherical explosion (curves 2). The recalculation was performed for values of R_1 larger or equal to $\sqrt{3/2}$ r (curves 1), the latter value corresponding to equality of gas mass in the sphere and in a cylinder limited by the tube walls and the shock wave front. In this case the shock wave parameters do not undergo a discontinuity at the point R_1, while at $R_1 > \sqrt{3/2}$ r they change discontinuously at the point of transition from spherical to planar symmetry, which may occur upon interaction of the direct shock-wave front with waves reflected from the walls.

Comparison of experimental data and curves 1, 2 show that R_1 increases with decrease in explosion energy concentration in the tube, which can be characterized by the parameter $M^{1/3}/r$. For example, for a charge M = 2.5 g at r = 1.5 cm the experimental data agree with the results of recalculating [2] within about 3% for $R_1 = \sqrt{3/2}$ r (Fig. 2), while for M = 0.8 g and r = 1.9 cm approximately the same accuracy is achieved at $R_1 = 3r$ (Fig. 3). The experimental data can be approximated by the function

$$R_1/r = \begin{cases} 5 - 0.42M^{1/3}/r, & 4 \leqslant M^{1/3}/r \leqslant 9 \ (\text{kg}^{1/3}/\text{m}), \\ \sqrt{3/2}, & M^{1/3}/r > 9 \ (\text{kg}^{1/3}/\text{m}). \end{cases} \quad (1)$$

The accuracy of this approximation is demonstrated by Fig. 4, which shows a hodograph (M = 0.8 g, r = 1.5 cm) for which the transition boundary R_1 was found with Eq. (1).

The process of formation of an intense planar shock wave in the tube is controlled by interaction of the direct and reflected waves. With distance the angle of shock-wave incidence upon the wall increases and at $\alpha = \alpha_* = (1/2) \arccos((\gamma - 1)/2)$ a transition from a regular reflection regime to irregular occurs, with formation of a three-wave configuration [3]. The point of intersection of the Mach wave with the direct shock wave shifts toward the tube axis, which then leads to formation of a planar shock wave in the tube at a distance $R_* \approx 4.7$ r (for the experimental conditions). With decrease in the intensity of the shock wave incident upon the tube wall R_* increases [3], which agrees with measurement results (Figs. 2-4). The further process of shock-wave formation is related to creation of planar

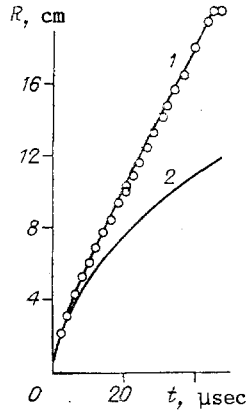

Fig. 2

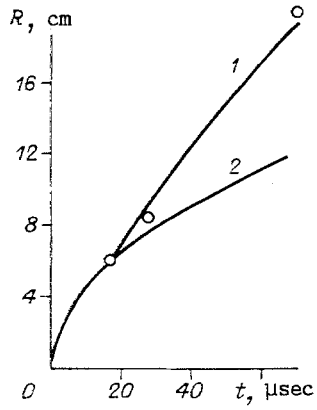

Fig. 3

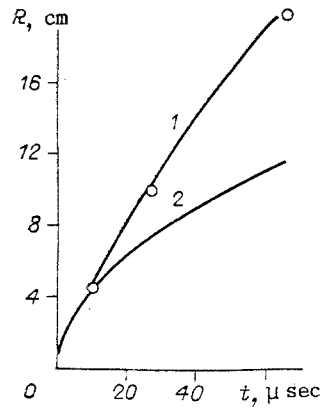

Fig. 4

waves upon collision of reflected waves on the tube axis and their interaction with the direct wave front ("overtaking").

The shock-wave front parameters in the tube can be found from its velocity, obtainable by graphical differentiation of the hodographs, and the shock adiabat of air [3], as was done in [2]. To obtain sufficient accuracy it is then necessary to average results of a large number of experiments, which insures good agreement of the experimental data of [2] with the numerical calculation results of [4]. Analysis reveals that for a limited amount of experimental data the accuracy in front parameter determination necessary for practical applications can be achieved by recalculating the results of [2], achieving best agreement of the measured and calculated shock-wave hodographs by variation of the parameter R_1. The empirical expressions found in this manner for the hodograph R(t), the front velocity N, and the pressure Δp for spherical and planar symmetry are as follows:

spherical shock wave:

$$0.053 \leqslant R/M^{1/3} \leqslant R_1/M^{1/3}(\text{m/kg}^{1/3}),\quad R/M^{1/3} = 0.053(1 + 2.88\cdot 10^5 t/M^{1/3})^{0.64},$$

$$N = 1880(R/M^{1/3})^{-0.56},\quad \Delta p = 3.8(R/M^{1/3})^{-1.14};$$

planar shock wave:

$$R_1/M \leqslant R/M \leqslant 0.0429/B\ (\text{m/kg}),$$

$$\frac{t-t_1}{R_1} = \frac{(BR_1/M)^{0.187}}{2232}\left[\left(\frac{R}{R_1}\right)^{1.187} - 1\right],\quad \frac{t_1}{M^{1/3}} = \frac{(R_1/R_0)^{1,56}-1}{2.88\cdot 10^5},$$

$$N = 1880(BR/M)^{-0.187},\quad \Delta p = 3.8(BR/M)^{-0.38};$$

$$R_2/M = 0.0429/B \leqslant R/M \leqslant 0.512/B\ (\text{m/kg}),$$

$$\frac{t-t_2}{R_2} = \frac{(BR_2/M)^{0,3}}{1664}\left[\left(\frac{R}{R_2}\right)^{1,3} - 1\right],\quad \frac{t_2-t_1}{R_1} = \frac{(BR_1/M)^{0.187}}{2232}\left[\left(\frac{R_2}{R_1}\right)^{1,187} - 1\right],$$

$$N = 1280(BR/M)^{-0.3},\quad \Delta p = 1.78(BR/M)^{-0,6};$$

$$R_3/M = 0.512/B \leqslant R/M \leqslant 4.096/B\ (\text{m/kg}),$$

$$\frac{t-t_3}{R_3} = \frac{(BR_3/M)^{0,377}}{1694}\left[\left(\frac{R}{R_3}\right)^{1,377} - 1\right],\quad \frac{t_3-t_2}{R_2} = \frac{BR_2/M^{0,3}}{1664}\left[\left(\frac{R_3}{R_2}\right)^{1,3} - 1\right],$$

$$N = 1230(BR/M)^{-0,377},\quad \Delta p = 1.42(BR/M)^{-0.85}.$$

Here R_0 is the explosive charge radius, $B = 1.5\ r^2$; R, r measured in m, M in kg; Δp in MPa, t in sec, N in km/sec. In the range $0.512 \leq BR/M$, where piston action of the explosion products ends, the pressure on the shock-wave front defined by the expressions presented above agrees with that calculated by the expression of [1] (dimensions of the quantities the same) $\Delta p = 7.87\cdot 10^{-7}\varepsilon/R + 3.9\cdot 10^{-4}\sqrt{\varepsilon/R}$ ($\varepsilon = MQ/(2\pi r^2)$). For TEN $Q = 5.9\cdot 10^6$ J/kg.

LITERATURE CITED

1. V. N. Rodionov, Yu. N. Ryabinin, and Yu. S. Vakhrameev, "Shock-wave attenuation in constant section channels," in: Explosion Physics, 5th ed. [in Russian], Akad. Nauk SSSR, Moscow (1956).

2. B. D. Khristoforov, "Shock-wave front parameters in air for explosions of charges of TEN and lead azide of various density," Zh. Prikl. Mekh. Tekh. Fiz., No. 6, (1961).
3. F. A. Baum, L. P. Orlenko, K. P. Stanyukovich, et al., Explosion Physics [in Russian] Nauka, Moscow (1975).
4. V. V. Koren'kov and V. N. Okhitin, "Numerical estimation of the effect of explosive charge density on air shock-wave parameters," Zh. Prikl. Mekh. Tekh. Fiz., No. 3 (1983).

PHASE TRANSITION KINETICS IN THE PRESENCE OF JOULEAN DISSIPATION

A. S. Pleshanov

UDC 537.528;537.529

A phase transition in the presence of volume heat liberation occurs in electrical breakdown of condensed media, in electrical explosion of conductors, and in various commutation processes. It was noted in [1, 2] that under conditions of volume heat liberation the phase transition includes a region of phase coexistence. However to the best of the author's knowledge the effect of volume heat liberation on the kinetics of the phase transition have yet to be studied. The present study will offer a theoretical analysis of this effect.

Let an electrical current of density j pass through a layer of condensed material. Due to Joulean dissipation the temperature T of the layer increases. The nonsteady-state T distribution can be found from the one-dimensional thermal conductivity equation

$$\rho w_t = (\varkappa T_x)_x + j^2/\sigma, \tag{1}$$

where $w = w^0 + cT$ is the enthalpy (w^0 is the reference level for measurement of w, c is the heat capacity); ρ is the density; $\varkappa$ is the thermal conductivity coefficient; σ is the electrical conductivity; x is the coordinate across the layer; the subscript denotes differentiation. The initial condition at time $t = 0$ has the form

$$T(x, 0) = T_0, \tag{2}$$

while the boundary condition corresponding to Newtonian heat exchange with the external medium at $T = T_0$ is

$$[\varkappa T_x + \alpha(T - T_0)]|_d = 0 \tag{3}$$

(where α is the heat exchange coefficient and d is the layer half-width). When T_{max} reaches the phase transition temperature T_* a new phase appears, the process of heat propagation within which is described by an equation analogous to Eq. (1). On the phase boundary the conditions of continuity of j, and the mass and energy fluxes are satisfied, as well as continuity of the potential φ and T:

$$\{j\} = \{\rho v\} = \{\rho v w - \varkappa T_x\} = 0, \{\varphi\} = \{T\} = 0. \tag{4}$$

Here v is the velocity relative to the seam and $\{f\} = f_2 - f_1$ (the subscripts $\alpha = 1, 2$ refer to the initial and new phases respectively). Sample φ and T distributions under conditions of identical heat exchange at both boundaries are shown in Fig. 1.

In fact, when T_{max} reaches the value T_* under the conditions of the given problem, where heat is conducted to the layer volumewise and at a finite rate, a finite time is required for transition of phase 1 into phase 2. There follows from Eq. (1) an expression describing this nonsteady-state process at $T_1 = T_2 = T_*$:

$$\rho w_{*t} = j^2/\sigma_*, \tag{5}$$

where $w_* = \sum_\alpha w_{\alpha *} x_\alpha = w_{1*} + (w_{2*} - w_{1*}) x_2 \equiv w_{1*} + \Delta w_* x_2$; $\sigma_* = \sum_\alpha \sigma_{\alpha *} x_\alpha = \sigma_{1*} + (\sigma_{2*} - \sigma_{1*}) x_2 \equiv \sigma_{1*} + \Delta\sigma_* x_2$; x_α is the volume concentration of the phase α, coinciding in view of the equality of the molecular weights of both phases with its mass fraction (it is assumed that σ_α is proportional to the volume density of charge carriers n); the subscript * indicates $T = T_*$. Here we use an additive expression for the conductivity of the mixture, which gives a minimum value

Moscow. Translated from Zhurnal Prikladnoi Mekhaniki i Tekhnicheskoi Fiziki, No. 5, pp. 28-33, September-October, 1988. Original article submitted May 18, 1987.

